Kent Academic Repository

Han, Zixiang, Ding, Haiyu, Han, Lincong, Ma, Liang, Zhang, Xiaozhou, Lou, Mengting, Wang, Yajuan, Jin, Jing, Wang, Qixing, Liu, Guangyi and and others (2024) *Cellular network based multistatic integrated sensing and communication systems.* IET Communications, 18 (20). pp. 1878-1888. ISSN 1751-8636.

IET Communications

ORIGINAL RESEARCH

Cellular network based multistatic integrated sensing and communication systems

Zixiang Han[1] ⓘ | Haiyu Ding[1] | Lincong Han[1] | Liang Ma[1] | Xiaozhou Zhang[1] |
Mengting Lou[1] | Yajuan Wang[1] | Jing Jin[1] | Qixing Wang[1] | Guangyi Liu[1] |
Jiangzhou Wang[2]

[1]China Mobile Research Institute, Beijing, China

[2]School of Engineering and Digital Arts, University of Kent, Canterbury, UK

Correspondence
Haiyu Ding, China Mobile Research Institute, Beijing 100053, China.
Email: dinghaiyu@chinamobile.com

Funding information
National Key Research and Development Program of China, Grant/Award Number: 2020YFB1806800

Abstract

A novel multistatic integrated sensing and communication (ISAC) system based on cellular network is proposed. It can make use of widespread base stations (BSs) to perform cooperative sensing in wide area. This system is important since the deployment of sensing function can be achieved upon the mobile communication network at low complexity and cost without modifying the architecture of BSs for full duplexing. In this work, the topology of sensing cell is first provided, which can be duplicated to seamlessly cover the cellular network. Each sensing cell consists of a single central BS transmitting signals and multiple neighboring BSs receiving reflected signals from sensing objects. Then an estimating approach is described for obtaining position and velocity of sensing objects that locate in the sensing cell. Joint data processing with an efficient optimization method is also provided. In addition, key issues in the cellular network based multistatic ISAC system are analyzed. Simulation results show that the multistatic ISAC system can reduce interference power by over 10 dBm and significantly improve position and velocity estimation accuracy of objects when compared with the monostatic ISAC system, demonstrating the effectiveness and promise of implementing the proposed system in the mobile network.

1 | INTRODUCTION

Mobile network has been revolutionized in the past few decades. It has been evolving from providing only voice service to supporting high-speed data transmission for massive users. The upcoming sixth generation (6G) mobile networks are envisioned to be the key enabler for instantaneous and unlimited connectivity for everything [1]. As a result, novel services and capabilities can be provided, including extended reality (XR), artificial intelligence (AI), computing, sensing etc. [2]. One of the key emerging capabilities in 6G network is sensing which is expected for the realization of various new use cases, such as target detection, environmental monitoring and action recognition, with large amounts of device-free objects [3, 4]. Due to the commonalities between the communication and sensing in terms of hardware and radio resources [5], an integrated sensing and communication (ISAC) system was recently proposed [6, 7].

In ISAC system, the waveform for wireless communication purpose is simultaneously utilized for sensing function. Therefore, considerable integration gain can be achieved on cost, spectral efficiency and energy efficiency. On the other hand, the channel for ISAC system is also dual-functional and its model is critical for the performance estimation of both functions [8, 9]. Specifically, the sensing function aims to extract object parameters from the information of propagation channel while the communication process needs to correctly transfer the data via propagation channel [10]. Hence, mutual benefits between sensing and communication can be achieved by fully exploiting results from both functions, for example, the transmit beamforming can be designed to achieve the optimal performance in both functions [11]. Experimental study has also been obtained to verify the practicality of ISAC system [12]. These natural advantages make the deployment of ISAC system more desired in the mobile network.

To implement ISAC system in the mobile network, one approach is using each single base station (BS) as transceiver to sense the surrounding environment and this is referred to as *monostatic sensing* [13, 14]. By transmitting the communication signal, the BS can receive the reflected signal from sensing objects at the same time [15]. Then the object parameters, including position and radial velocity, can be obtained by estimating the angle of departure (AoD), angle of arrival (AoA), time delay and Doppler frequency etc. [16]. However, a full-duplex BS is required to accomplish the monostatic sensing while it is a currently immature technique [17]. In the mobile network with time-division duplexing (TDD) mode, an additional receiver for sensing function can be implemented with spatial isolation to the original transmitter on the same BS while the total size, cost and complexity of BSs are significantly increased. Moreover, the power of the self-interference (SI) due to BS self transmission and the mutual interference (MI) from the other neighboring BSs is strong in cellular network with monostatic sensing, resulting in degraded sensing performance. Therefore, it is a great burden for operators to deploy monostatic sensing in the cellular network.

To address the issues in monostatic sensing, *bistatic sensing* utilizing two BSs was proposed where one BS acts as transmitter with the other one being receiver [18–20]. This avoids the requirement of full duplexing and no further hardware change is necessary for BSs. Owing to the long distance between BSs, SI is automatically addressed. Besides, the number of BSs that transmit signals is reduced by half when incorporating bistatic sensing into cellular network, which can efficiently suppress the MI. However in bistatic sensing, there is always a blind zone where significant position estimation error occurs for objects located in this area [21]. In addition, similar to the monostatic sensing, the bistatic sensing is unable to fully recover the information of velocity [21]. As further extension of bistatic sensing and to overcome the challenges in both monostatic and bistatic sensing, in this work we propose a novel multistatic ISAC system based on cellular network. In this system, multiple BSs form a sensing cluster to perform *multistatic sensing* [22] where sensing results of multiple BS receivers can be jointly processed to improve sensing performance. To the best of our knowledge, an analysis of the multistatic sensing in cellular network has not been performed in the literature. The main contributions of this work are summarized as follows:

1) Proposing multistatic ISAC system in cellular network. With novel sensing cell structure, the proposed system overcomes the issues in monostatic and bistatic sensing, satisfying the requirement of large-scale ISAC implementation for operators.
2) Proposing an efficient approach with joint data optimization method to estimate position and velocity of sensing objects.
3) Analyzing and discussing key issues, including synchronization, uplink/downlink frame structure and interference in the proposed system.
4) Demonstrating the proposed multistatic ISAC system by simulating the interference power in the system and the error

of position and velocity estimation. It is shown that the proposed multistatic ISAC system can effectively suppress the interference power and improve the object estimation accuracy when compared with the monostatic ISAC system.

This article is organized as follows. Section 2 formulates the multistatic ISAC system model in cellular network. Section 3 describes an efficient estimation method for obtaining position and velocity of sensing objects. Section 4 analyzes key issues of the proposed system. Section 5 provides simulation results to demonstrate effectiveness of the proposed multistatic ISAC system. Section 6 concludes the work.

Notation. Bold lower and upper case letters denote vectors and matrices, respectively. Upper case letters in calligraphy denote sets. Letters not in bold font represent scalars. $|a|$ and $E[a]$ refer to the modulus and expectation of a scalar a. $[\mathbf{a}]_i$ and $\|\mathbf{a}\|$ refer to the ith element and l_2-norm of vector $\mathbf{a}$, respectively. $\mathbf{A}^T$ and $\mathbf{A}^H$ refer to the transpose and conjugate transpose of matrix $\mathbf{A}$, respectively. $\mathbb{C}$ denotes the complex number set. $j = \sqrt{-1}$ denotes imaginary unit.

2 | SYSTEM MODEL

2.1 | Sensing cell in cellular network

For monostatic ISAC system, as illustrated in Figure 1a, all BSs work in the same uplink (UL) or downlink (DL) mode at certain time, which is consistent with communication settings in TDD cellular network. However, BSs simultaneously transmit and receive signals for sensing purpose so that each BS receives both SI signal from itself and MI signals from all the other BSs. To avoid SI and MI issue in monostatic sensing, we consider multistatic ISAC system where BSs work in different modes. In general, smaller proportion of BSs in the DL mode is more beneficial for MI suppression. Thus as shown in Figure 1b, partial BSs in the DL mode transmit signals to surrounding environment with the other BSs in the UL mode receiving the reflected signals from objects.

To analyze the multistatic ISAC system in Figure 1b, we discretize cellular network into multiple fragment of sensing cells as enclosed by blue line in Figure 2. In the sensing cell, a single BS with 3 panels locates at the center, each panel has N antennas as transmitter covering a sector of the sensing cell. In addition, panels of BSs in the neighboring cells, facing towards the central BS, act as receivers in the sensing cell. Receivers are rotationally symmetrical about the transmitter and the structure of the sensing cell has both rotational and axial symmetries. Therefore, it is straightforward to note that the sensing cell can be duplicated and transformed to seamlessly cover the cellular network. In addition with the sensing cell structure, only one-third of the BSs in cellular network work in the DL mode for sensing function, resulting in lower MI power. The overall interference of the cellular network with this sensing cell structure will be presented in the simulation section.
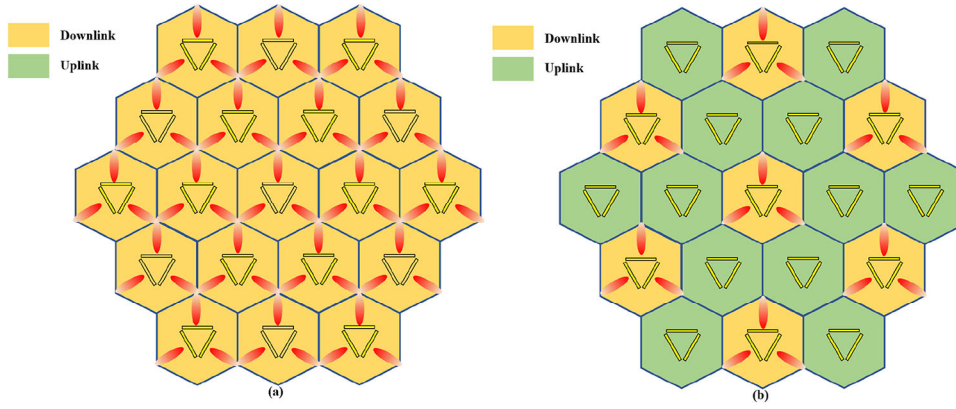
FIGURE 1 Examples of UL/DL status of BSs in (a) monostatic (b) multistatic ISAC system based on cellular network.
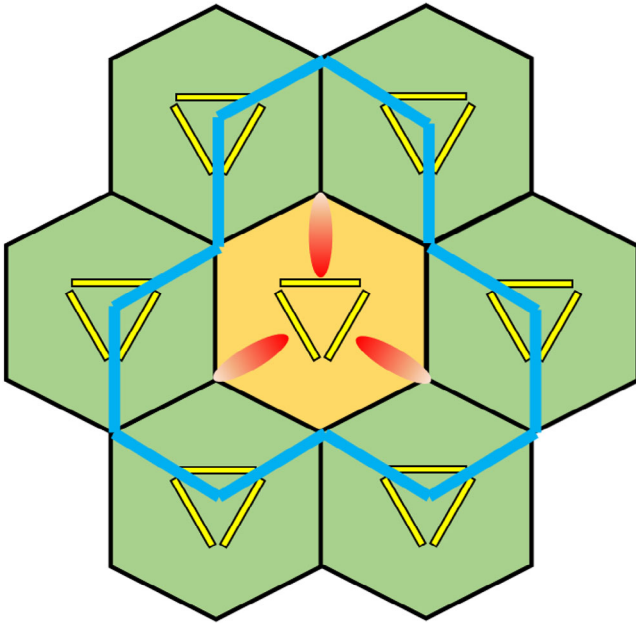

FIGURE 2 Structure of sensing cell in multistatic ISAC system.

2.2 | Signal model

The transmitted signal on the nth transmit antenna is in the form of orthogonal frequency division multiplexing (OFDM) signals [23, 24] given by

$$x_n(t) = \sum_{n_s=0}^{N_s-1} \sum_{n_c=0}^{N_c-1} s_n(n_c, n_s) e^{j2\pi f_\Delta n_c t} r(t - n_s T_s), n = 1, 2, \cdots, N,$$

$$(1)$$

where N_c and N_s are the numbers of subcarriers and OFDM symbols, respectively. $s_n(n_c, n_s)$ is the modulated symbol on the n_cth subcarrier of the n_sth OFDM symbol at the nth transmit antenna. f_Δ is the subcarrier spacing, T_s is the OFDM symbol period including cyclic prefix, $r(t)$ is the function of pulse shaping filter. The received frequency-domain symbols (with matched filtering) of the kth receiver, $k = 1, 2, \ldots, K$, in the

sensing cell can be written as

$$\mathbf{y}_k(n_c, n_s) = \mathbf{H}_k(n_c, n_s)\mathbf{s}(n_c, n_s) + \mathbf{n}_k(n_c, n_s) + \mathbf{i}_k(n_c, n_s), \quad (2)$$

where $\mathbf{y}_k(n_c, n_s) = [y_{k,1}(n_c, n_s), y_{k,2}(n_c, n_s), \ldots, y_{k,N}(n_c, n_s)]^T \in \mathbb{C}^{N \times 1}$ is the received symbol vector with $y_{k,n}(n_c, n_s)$ being the received symbol on the n_cth subcarrier of the n_sth OFDM symbol at the nth receive antenna of the kth receiver. $\mathbf{n}_k \in \mathbb{C}^{N \times 1}$ and $\mathbf{i}_k \in \mathbb{C}^{N \times 1}$ are the additive noise and interference signal. $\mathbf{s}(n_c, n_s) = [s_1(n_c, n_s), s_2(n_c, n_s), \ldots, s_N(n_c, n_s)]^T \in \mathbb{C}^{N \times 1}$ is the transmitted frequency-domain symbol vector. $\mathbf{H}_k(n_c, n_s) \in \mathbb{C}^{N \times N}$ is the frequency-domain channel given by

$$\mathbf{H}_k(n_c, n_s) = \sum_{l=1}^{L} \beta_{k,l} e^{j2\pi T_s f_{D,k,l} n_s} e^{-j2\pi \tau_{k,l} f_\Delta n_c} \mathbf{a}_{R,k}(\Omega_{R,k,l})$$

$$\times \mathbf{a}_T^T(\Omega_{T,l}), \quad (3)$$

where L is the number of sensing objects, $\beta_{k,l} \in \mathbb{C}$ is the channel gain of the lth path, $\tau_{k,l} = \frac{d_{k,l}}{c}$ is the time delay with $d_{k,l}$ and c referring to the signal propagation distance and light speed. Specifically, $d_{k,l} = d_{T,l} + d_{R,k,l}$ where $d_{T,l}$ and $d_{R,k,l}$ are the signal propagation distances from the transmitter to the lth object and from the lth object to the kth receiver [25]. $f_{D,k,l} = \frac{v_{\parallel,k,l} f_c}{c}$ is the Doppler frequency of the lth object with $v_{\parallel,k,l}$ and f_c denoting projected velocity and carrier frequency, respectively. In particular, the projected velocity $v_{\parallel,k,l}$ can be decomposed as $v_{\parallel,k,l} = v_{\parallel,R,k,l} + v_{\parallel,T,l}$ where $v_{\parallel,R,k,l}$ and $v_{\parallel,T,l}$ are the radial velocities of the lth object with respect to the kth receiver and the transmitter [25]. $\mathbf{a}_{R,k}(\Omega_{R,k,l}) \in \mathbb{C}^{N \times 1}$ and $\mathbf{a}_T(\Omega_{T,l}) \in \mathbb{C}^{N \times 1}$ are the steering vectors of the receive antennas and the transmit antennas, respectively, $\Omega_{R,k,l}$ and $\Omega_{T,l}$ are angle of arrival (AoA) and angle of departure (AoD) of the lth path. $\mathbf{H}_k$ can be written as $\mathbf{H}_k = [\mathbf{h}_{k,1}, \mathbf{h}_{k,2}, \ldots, \mathbf{h}_{k,N}]$ with $\mathbf{h}_{k,n} \in \mathbb{C}^{N \times 1}$ being the channel related to the nth transmit antenna in the frequency domain. It should be noted that to estimate the channel parameters related to sensing objects, that is, $f_{D,k,l}$, $\tau_{k,l}$, and $\Omega_{R,k,l}$, the modulated symbol vector

s is normally chosen as communication reference signal that known to all receivers. Then the channel parameters, estimated by all receivers, are sent to server for further joint processing to determine position and velocity of sensing objects. This will be described in the next section.

3 | MULTISTATIC SENSING

In this section, we present an efficient approach to estimating position and velocity of sensing objects in multistatic ISAC system.

3.1 | Channel parameters estimation

We start with estimating AoA of the received signal. In this work, we consider the multistatic sensing on the azimuth plane (with azimuth angle ϕ) as an illustrative example. Assuming AoA remains unchanged within N_s OFDM symbol period, from (2) we define

$$g_k(\phi, n_c, n_s) = \mathbf{a}_{R,k}^H(\phi)\mathbf{y}_k(n_c, n_s), \ \phi \in \Phi_k, \tag{4}$$

where Φ_k is the AoA range for the kth receiver in the sensing cell. Then we calculate the sum power for all N_c subcarriers in N_s OFDM symbol period as

$$h_k(\phi) = \sum_{n_s=0}^{N_s-1} \sum_{n_c=0}^{N_c-1} \left| g_k(\phi, n_c, n_s) \right|^2. \tag{5}$$

Generally when $\phi = \phi_{R,k}$, $\phi \in \Phi_k$, (2) can be perfectly compensated for $\mathbf{a}_{R,k}(\phi)$ so that (5) reaches local maximum value. Therefore, AoA set $\hat{\Phi}_{R,k}$ can be obtained by searching the peaks of $h_k(\phi)$.

Next we estimate signal propagation distance and projected velocity based on g_k in (4) and the estimated AoA. Using each stream of modulated symbol s_n to divide g_k, we have

$$\tilde{g}_{k,n}(\phi, n_c, n_s) = \frac{g_k(\phi, n_c, n_s)}{s_n} = \mathbf{a}_{R,k}^H(\phi)\mathbf{h}_{k,n}(n_c, n_s)$$
$$+ \mathbf{a}_{R,k}^H(\phi)\tilde{\mathbf{n}}_k(n_c, n_s), \phi \in \hat{\Phi}_{R,k}, \tag{6}$$

where $\tilde{\mathbf{n}}_k(n_c, n_s) = \frac{\mathbf{n}_k(n_c,n_s)+\mathbf{i}_k(n_c,n_s)}{s_n(n_c,n_s)}$ refers to the ratio of interference plus noise to the transmitted symbol. To extract the information of time delay and projected velocity from (6), we can perform two dimension (2D) discrete Fourier transform (DFT) on $\tilde{g}_{k,n}$ [26] as

$$\tilde{G}_{k,n}(p, q) = \frac{1}{N_c N_s} \sum_{n_s=0}^{N_s-1} \sum_{n_c=0}^{N_c-1} \tilde{g}_{k,n}(\phi, n_c, n_s)$$
$$\times e^{-j\left(p-\frac{N_s}{2}\right)\frac{2\pi}{N_s}n_s} e^{j(q-1)\frac{2\pi}{N_c}n_c}, \tag{7}$$

where N_s is assumed to be even. The peaks in $\tilde{G}_{k,n}(p, q)$, indexed by $(\hat{p}_{k,n}, \hat{q}_{k,n})$, are derived for estimating time delay and projected velocity of the propagation path as

$$T_s f_D = \frac{\left(\hat{p}_{k,n} - \frac{N_s}{2}\right)}{N_s}, \tag{8}$$

$$\tau f_\Delta = \frac{\left(\hat{q}_{k,n} - 1\right)}{N_c}. \tag{9}$$

The propagation distance $\hat{d}_{k,n}$ and the projected velocity $\hat{v}_{\parallel,k,n}$ of sensing objects can then be solved as

$$\hat{v}_{\parallel,k,n} = \frac{\left(\hat{p}_{k,n} - \frac{N_s}{2}\right)c}{N_s T_s f_c}, \tag{10}$$

$$\hat{d}_{k,n} = \frac{\left(\hat{q}_{k,n} - 1\right)c}{N_c f_\Delta}. \tag{11}$$

It should be noted that (6) to (11) can be repeated for each s_n, $n = 1, 2, \ldots, N$, and we can thus average $\hat{d}_{k,n}$ and $\hat{v}_{\parallel,k,n}$, $n = 1, 2, \ldots, N$, that is, $\hat{d}_k = \frac{1}{N}\sum_{n=1}^N \hat{d}_{k,n}$ and $\hat{v}_{\parallel,k} = \frac{1}{N}\sum_{n=1}^N \hat{v}_{\parallel,k,n}$, as the estimated propagation distance and projected velocity by the kth receiver. To this end, the estimated channel parameters of sensing objects $(\hat{\phi}_{R,k}, \hat{d}_k, \hat{v}_{\parallel,k})$ can be obtained.

We provide here brief expressions of the estimation error on $(\hat{\phi}_{R,k}, \hat{d}_k, \hat{v}_{\parallel,k})$. For the estimation of AoA, the error $\phi^e = |\hat{\phi}_{R,k} - \phi_{R,k}|$ depends on the resolution of ϕ in (4), denoted by $\Delta\phi$, and its expectation is $E[\phi^e] = \frac{\Delta\phi}{4}$. This is because ϕ^e is uniformly distributed within $[0, \frac{\Delta\phi}{2}]$. Similarly, the resolution of projected velocity and signal propagation distance are, respectively, given by $\Delta v_\parallel = \frac{c}{N_s T_s f_c}$ and $\Delta d = \frac{c}{N_c f_\Delta}$. Therefore, the expectation for estimation error of projected velocity and signal propagation distance are $E[v_\parallel^e] = \frac{c}{4N_s T_s f_c}$ and $E[d^e] = \frac{c}{4N_c f_\Delta}$ which are inversely proportional to the total OFDM symbol duration $N_s T_s$ and system bandwidth $N_c f_\Delta$, respectively.

3.2 | Position and velocity estimation

In this subsection, we estimate position and velocity of sensing objects based on the estimated AoA $\hat{\phi}_{R,k}$, signal propagation distance $\hat{d}_k$ and projected velocity $\hat{v}_{\parallel,k}$ for $k = 1, 2, \ldots, K$. As shown in Figure 3, assuming the coordinate of transmitter is (x_0, y_0) and the distance between transmitter and receiver is d_0, the location of receivers in the sensing cell are given by $(x_k, y_k) = (x_0 + d_0\cos(\frac{2k-1}{K}\pi), y_0 + d_0\sin(\frac{2k-1}{K}\pi))$ for $k = 1, 2, \ldots, K$.

3.2.1 | Position estimation

We first estimate object positions using AoA $\hat{\phi}_{R,k}$ and propagation distance $\hat{d}_k$, $k = 1, 2, \ldots, K$. There are two estimation
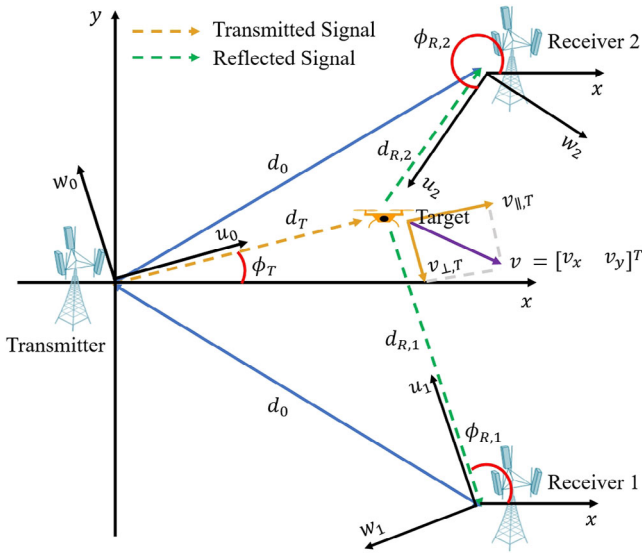
FIGURE 3 Illustration of position and velocity estimation method in cellular network.

methods that are related to different data fusion strategies: (1) Hard data fusion: each receiver estimates and sends the object position to server for calculating the weighted mean position [21]. This method is referred to as mean position method (MPM) and is most suitable for the scenarios where computing resources at the server is tight. (2) Soft data fusion: all receivers send AoA $\hat{\phi}_{R,k}$ and propagation distance $\hat{d}_k$ to server for joint optimization to estimate object positions. In this work, we mainly focus on the second method while the performance comparison between two methods is provided in the simulation section.

Assuming the coordinate of object position is (x, y), we define the loss function for position estimation as

$$f_{\text{pos}}(x, y) = \frac{\sum_{k=1}^{K} \alpha_k |\hat{d}_k - d_T - d_{R,k}|}{\sum_{k=1}^{K} \alpha_k} + \frac{\sum_{k=1}^{K} \beta_k |\hat{\phi}_{R,k} - \phi_k|}{\sum_{k=1}^{K} \beta_k},$$

(12)

where $d_T = \sqrt{(x - x_0)^2 + (y - y_0)^2}$ is the distance between the transmitter and the object, $d_{R,k} = \sqrt{(x - x_k)^2 + (y - y_k)^2}$ is the distance between the object and the kth receiver, $\phi_k = \arctan\frac{y - y_k}{x - x_k}$ is the angle of object with respect to the kth receiver. α_k and β_k are the weighting coefficients for the kth receiver. To determine the value of α_k and β_k, we consider the signal power at the kth receiver side. The received signal power is inversely proportional to $d_T^2 d_{R,k}^2$ [6] so that we let $\alpha_k = d_T^{-2} d_{R,k}^{-2}$. On the other hand, the position estimation error due to the AoA estimation error can be approximated as $d_{R,k}|\hat{\phi}_{R,k} - \phi_k|$. Thus, we define $\beta_k = \alpha_k d_{R,k} = d_T^{-2} d_{R,k}^{-1}$. It is expected that AoA and propagation distance associated to the object at location (x, y) are closest to the estimated parameters $\hat{\phi}_{R,k}$ and $\hat{d}_k$. Therefore,

the optimization problem can be formulated as

$$\min_{x, y} f_{\text{pos}}(x, y).$$

(13)

The problem (13) is an unconstrained optimization problem. Therefore, efficient optimization algorithms, such as quasi-Newton method [27], can be used to solve (13).

To help find an optimal solution that is close to the global optimum and support convergence, it is important to provide a good initial point for the quasi-Newton method. Specifically, we can use two AoA $\hat{\phi}_{R,k_1}$ and $\hat{\phi}_{R,k_2}$ estimated by the k_1th and the k_2th receivers together with receiver location (x_{k_1}, y_{k_1}) and (x_{k_2}, y_{k_2}), $k_1, k_2 = 1, 2, \dots, K$, $k_1 \neq k_2$ to derive the initial guess of object position as

$$x_{\text{init}} = \frac{y_{k_2} - y_{k_1} + \tan(\hat{\phi}_{R,k_1}) x_{k_1} - \tan(\hat{\phi}_{R,k_2}) x_{k_2}}{\tan(\hat{\phi}_{R,k_1}) - \tan(\hat{\phi}_{R,k_2})},$$

(14)

$$y_{\text{init}} = \frac{x_{k_2} - x_{k_1} + \cot(\hat{\phi}_{R,k_1}) y_{k_1} - \cot(\hat{\phi}_{R,k_2}) y_{k_2}}{\cot(\hat{\phi}_{R,k_1}) - \cot(\hat{\phi}_{R,k_2})}.$$

(15)

Using initial object position $(x_{\text{init}}, y_{\text{init}})$, we can derive $d_{T,\text{init}}$ and $d_{R,k,\text{init}}$ as the initial distance between the object and the transmitter as well as the kth receiver. The initial AoA is $\phi_{k,\text{init}} = \arctan\frac{y_{\text{init}} - y_k}{x_{\text{init}} - x_k}$. The initial values for $\alpha_{k,\text{init}} = d_{T,\text{init}}^{-2} d_{R,k,\text{init}}^{-2}$ and $\beta_{k,\text{init}} = d_{T,\text{init}}^{-2} d_{R,k,\text{init}}^{-1}$ can also be obtained. By using the proposed optimization method, the optimal estimation of object position can be rapidly obtained as $(\hat{x}, \hat{y})$.

3.2.2 | Velocity estimation

Next, we estimate object velocity $\mathbf{v} = [v_x, v_y]^T$ based on the estimated object position $(\hat{x}, \hat{y})$ and the projected velocity $\hat{v}_{\parallel,k}$, $k = 1, 2, \dots, K$. To perform the estimation, we need to first find the relationship between $\hat{v}_{\parallel,k}$ and $\mathbf{v}$. Since the projected velocity $\hat{v}_{\parallel,k}$ is composed by two radial velocities $\hat{v}_{\parallel,T}$ and $\hat{v}_{\parallel,R,k}$, we set up local coordinate to obtain $\hat{v}_{\parallel,T}$ and $\hat{v}_{\parallel,R,k}$ as a function of object velocity $\mathbf{v}$. As shown in Figure 3, the local coordinate (u, w) are set with the origin being the position of transmitter or receiver and the positive u-axis pointing from the origin to the object. The coordinate transformation from global coordinate to local coordinate can be expressed by matrix

$$\mathbf{T}(\phi) = \begin{bmatrix} \cos(\phi) & \sin(\phi) \\ -\sin(\phi) & \cos(\phi) \end{bmatrix}.$$

(16)

As shown in Figure 3, by decomposing $\mathbf{v}$ in the local coordinate of the transmitter, that is, (u_0, w_0)-coordinate, we can obtain $\mathbf{v}_T = [v_{\parallel,T}, v_{\perp,T}]^T$ where $v_{\parallel,T}$ and $v_{\perp,T}$ are referred to as the radial and tangential velocity of object with respect to the transmitter. Similar decomposition can be performed on $\mathbf{v}$ in the (u_k, w_k)-coordinate of the kth receiver and we obtain $\mathbf{v}_{R,k} = [v_{\parallel,R,k}, v_{\perp,R,k}]^T$ where $v_{\parallel,R,k}$ and $v_{\perp,R,k}$ are referred to as the radial and tangential velocity of object with respect to the

kth receiver. We can relate the velocities in local coordinates and in global coordinate by

$$\mathbf{v}_T = \mathbf{T}(\hat{\phi}_T)\mathbf{v}, \tag{17}$$

$$\mathbf{v}_{R,k} = \mathbf{T}(\hat{\phi}_{R,k})\mathbf{v}, \tag{18}$$

where $\hat{\phi}_T = \arctan\frac{\hat{y}-y_0}{\hat{x}-x_0}$ and $\hat{\phi}_{R,k} = \arctan\frac{\hat{y}-y_k}{\hat{x}-x_k}$. Based on (17) and (18), the relationship between the projected velocity $v_{\parallel,k}$ and the object velocity $\mathbf{v}$ can be derived as

$$v_{\parallel,k} = v_{\parallel,T} + v_{\parallel,R,k} = \mathbf{w}_k^T \mathbf{v}, \tag{19}$$

where $\mathbf{w}_k = [w_{x,k}, w_{y,k}]^T$ with $w_{x,k} = \cos(\hat{\phi}_{R,k}) + \cos(\hat{\phi}_T)$ and $w_{y,k} = \sin(\hat{\phi}_{R,k}) + \sin(\hat{\phi}_T)$. With (19) we can define the loss function for velocity estimation as

$$f_{\text{vel}}(\mathbf{v}) = \frac{\sum_{k=1}^{K} \hat{\alpha}_k |\hat{v}_{\parallel,k} - v_{\parallel,k}|}{\sum_{k=1}^{K} \hat{\alpha}_k}, \tag{20}$$

where $\hat{\alpha}_k = \hat{d}_T^{-2}\hat{d}_{R,k}^{-2}$ with $\hat{d}_T$ and $\hat{d}_{R,k}$ being the distances between the estimated object position $(\hat{x}, \hat{y})$ and the transmitter as well as the kth receiver. The corresponding optimization problem can be formulated as

$$\min_{\mathbf{v}} f_{\text{vel}}(\mathbf{v}). \tag{21}$$

The optimization problem (21) can be solved again by using quasi-Newton method.

We also provide a good initial guess for object velocity $\mathbf{v}_{\text{init}} = [v_{x,\text{init}}, v_{y,\text{init}}]^T$. This can be derived by collecting two estimated projected velocities into vector $\hat{\mathbf{v}}_{\parallel,k_1,k_2} = [\hat{v}_{\parallel,k_1}, \hat{v}_{\parallel,k_2}]^T$, $k_1, k_2 = 1, 2, \ldots, K$, $k_1 \neq k_2$ and using (19) as

$$\mathbf{v}_{\text{init}} = \begin{bmatrix} \mathbf{w}_{k_1} & \mathbf{w}_{k_2} \end{bmatrix}^{-T} \hat{\mathbf{v}}_{\parallel,k_1,k_2}. \tag{22}$$

By using quasi-Newton method, the optimal estimation of object velocity $\mathbf{v} = [\hat{v}_x, \hat{v}_y]^T$ can be obtained. Note that monostatic and bistatic sensing system cannot fully recover the velocity of object $\mathbf{v}$.

Algorithm 1 summarizes the overall method for estimating position and velocity of sensing objects. The performance is verified in the simulation section.

4 | KEY ISSUES

In this section, we analyze and discuss key issues in multistatic ISAC system in cellular network, including time synchronization, uplink/downlink frame structure and interference.

4.1 | Time synchronization

Synchronization issue is critical in any mobile communication system. In multistatic ISAC system, the estimation accuracy of

ALGORITHM 1 The optimization method for position and velocity estimation.

**Input:** $\hat{\phi}_{R,k}, \hat{d}_k, \hat{v}_{\parallel,k}, k = 1, 2, \ldots, K$;
  1: Find x_{init} and y_{init} by (14) and (15);
  2: Find $d_{T,\text{init}}, d_{R,k,\text{init}}$, and $\phi_{k,\text{init}}$ using x_{init} and y_{init};
  3: Find $(\hat{x}, \hat{y})$ by (13);
  4: Find $\hat{d}_T, \hat{d}_{R,k}, \hat{\phi}_{R,k}$, and $\hat{\phi}_T$ using $(\hat{x}, \hat{y})$ in step 3;
  5: Find $v_{\parallel,T}$ and $v_{\parallel,R,k}$ by (17) and (18);
  6: Find $\mathbf{v}_{\text{init}}$ by (19) and (22);
  7: Find $\hat{\mathbf{v}}$ by (21);
Output: $(\hat{x}, \hat{y})$ and $\hat{\mathbf{v}}$;

---

signal propagation distance $\hat{d}_k$ and resulting positioning accuracy strongly depend on the time synchronization error among BSs. For example, the BS synchronization error in current BS protocol TS 38.133 [28] shall not exceed 3 ¯s, indicating that the estimation error of $\hat{d}_k$ due to asynchronization can reach 900 m which is totally unacceptable. To reduce the synchronization error, global navigation satellite system is one solution where few-nanosecond asynchronization can be achieved [29] and the consequent estimation error of $\hat{d}_k$ is below 3 m. For higher-precision positioning, one approach is to obtain synchronization error among BSs to mitigate estimation error of $\hat{d}_k$. This can be performed by round-trip transmission for each pair of BSs in the cellular network. The time delay difference between the forward and the backward propagation in the round-trip transmission can be utilized to calculate synchronization error. However, this approach is exhaustive and time-consuming when the number of BSs to be synchronized is large. Another approach avoids BS synchronization error issue by estimating object position without using signal propagation distance $\hat{d}_k$. That is, the position estimation can purely depends on the estimation of AoA and the term related to distance in (13) can be dropped. This approach is preferred when object association can be performed.

4.2 | UL/DL frame structure

As shown in Figure 1b, the UL/DL status of BSs are different in the multistatic ISAC system, which is inconsistent with the communication settings as in Figure 1a. To realize multistatic sensing in TDD cellular network, dedicated symbols or slots have to be allocated by receivers to receive the reflected signal from sensing objects. Therefore, the frame structure for transmitters (DL) and receivers (UL) are different. One frame design with least modification to the original frame structure is to tune the DL/UL symbol ratio in flexible slot for transmitters and receivers. An illustrative example is provided in Figure 4a where the sensing function is performed during the sensing period of few symbols time. However, an elongated sensing duration is desired for velocity estimation whose error is associated to the total OFDM symbol period as described in Section 3. A. To that end, a double-function slot can be designed in new frame
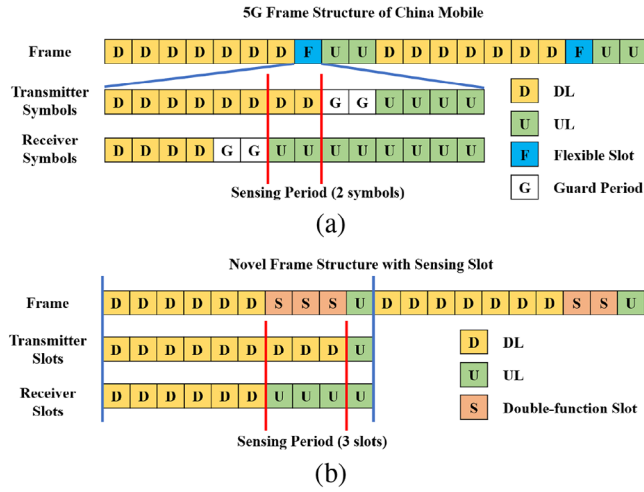
FIGURE 4 Illustrative examples of UL/DL frame structure for sensing purpose in cellular network.

structure for multistatic ISAC system as illustrated in Figure 4b. That is, the double-function slot is activated for sensing purpose when sensing service is prior to communication service.

4.3 | Interference

It is also important to analyze the interference issue in the multistatic ISAC system. We also analyze the interference in the monostatic ISAC system as comparison.

One of the major interference signals received by a single receiver in multistatic ISAC system is mutual interference (MI) from the DL BSs in the non-adjacent sensing cells. Particularly, MI power is higher as the number of BSs in the DL mode increases. For our proposed sensing cell structure, the ratio of DL to UL BSs in cellular network is $\frac{1}{2}$ so that MI power is lower than that in monostatic ISAC system where all BSs simultaneously transmit and receive signals for sensing purpose.

On the other hand, user interference (UI) from the user equipments (UEs) in the UL mode can also be received in the multistatic ISAC system due to the co-existence of sensing and communication. However, when the power difference between the received UL communication signals from UEs and the received reflected signals from sensing objects is smaller than the maximum dynamic range of analog-to-digital converters (ADC), the received UL communication signals can be deleted from the overall received signals using method as successive interference cancellation. To meet the requirement of ADC, the uplink power control of UEs is needed. Another way to address this issue is using different subcarriers or resource group for sensing and communication, which also performs a tradeoff between the sensing and communication performance since the bandwidth for sensing determines the estimation error of object parameters. Instead of interfered by UEs in the multistatic ISAC system, BSs in the monostatic ISAC system suffer from self-interference (SI). The power difference between SI and the reflected signals from objects should be smaller than

TABLE 1 System parameters of cellular networks.

Parameters	Set 1	Set 2
Carrier frequency f_c (GHz)	2.6	26
Subcarrier spacing f_Δ (kHz)	30	120
System bandwidth BW (MHz)	100	400
OFDM symbol period T_s (ms)	0.0357	0.0089

the maximum dynamic range of ADC so that SI cancellation technique can be utilized [30].

The overall interference power in the multistatic and monostatic ISAC system will be provided in the next section.

5 | SIMULATION RESULTS

In the simulation, we consider two types of cellular networks, including the existing low-frequency mobile network and the future high-frequency millimeter wave mobile network. The system parameters are listed in Table 1. In addition, we consider quadrature phase shift keying (QPSK) modulated symbols on each subcarrier and $N = 16$ antennas with half-wavelength separation are utilized in each panel of transmitter and receiver.

5.1 | Interference

We first estimate the received interference power for a single BS receiver in the proposed multistatic ISAC system, which consists of MI from the DL BSs in the non-adjacent sensing cells and UI from UEs in the UL mode. In the simulation, the number of UEs is assumed as 500 in each cell. The transmit power of BSs and UEs are 43 dBm and 23 dBm, respectively. The system-level simulation results are provided in Table 2, which are also benchmarked with monostatic ISAC system in cellular network. It should be noted that in the monostatic ISAC system, UEs are in the DL mode so that there is no UI in this case.

It can be observed from Table 2 that for both low-frequency and high-frequency cellular networks, MI power in the multistatic ISAC system is 10 dB lower than that in the monostatic system for all BS distances. This is because the number of DL BSs in the proposed multistatic ISAC system is smaller. In addition, UI in the multistatic ISAC system is also smaller than mean SI in the monostatic ISAC system [31]. Therefore, the overall interference power in the multistatic ISAC system is lower than that in the monostatic ISAC system, demonstrating that the multistatic ISAC system can effectively suppress interference power.

5.2 | Positioning and velocity estimation performance

To further highlight the advantages of the proposed multistatic ISAC system, the performance of position and velocity

TABLE 2 Simulated interference power in multistatic and monostatic systems.

BS distance (m)	2.6 GHz						26 GHz					
	Multistatic (dBm)			Monostatic (dBm)			Multistatic (dBm)			Monostatic (dBm)		
	MI	UI	Overall	MI	SI	Overall	MI	UI	Overall	MI	SI	Overall
100	−32	−32	−29	−22	−27	−21	−50	−48	−47	−40	−48	−39
200	−38	−39	−36	−28	−27	−25	−56	−56	−53	−47	−48	−45
300	−42	−43	−40	−32	−27	−26	−60	−58	−56	−50	−48	−46
500	−47	−45	−43	−37	−27	−27	−65	−59	−58	−55	−48	−47
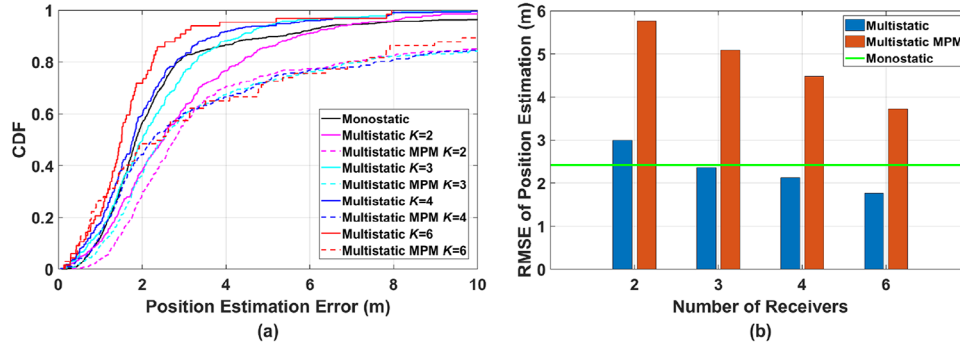
FIGURE 5 Simulated (a) CDF and (b) RMSE of position estimation in the proposed multistatic ISAC system based on 2.6 GHz cellular network.

estimation in terms of the cumulative distribution function (CDF) and root mean square error (RMSE) are simulated. We consider a single object located in the sensing cell and utilize results from K receivers, including AoA, signal propagation distance and projected velocity, for joint processing to obtain the estimated position and velocity as described in Section 3. B. The distance between BSs is assumed as $d_0 = 300$ m when $f_c = 2.6$ GHz and $d_0 = 100$ m when $f_c = 26$ GHz. In addition, the resolution of ϕ in (4) is set as $\Delta\phi = 1°$. Particularly, the resolution of projected velocity is inversely proportional to carrier frequency so that the number of OFDM symbols required for velocity estimation in $f_c = 2.6$ GHz system is very large. Therefore, we only estimate the velocity in multistatic ISAC system with $f_c = 26$ GHz where object velocity ranges from 5 to 35 m/s with arbitrary direction.

5.2.1 | Position estimation performance

As shown in Figure 5, the CDF of position estimation error as well as the RMSE, based on the joint optimization method, in the proposed multistatic ISAC system (referred to as Multistatic) based on 2.6 GHz cellular network are simulated, which are also benchmarked with the performance of monostatic ISAC system (referred to as Monostatic) and the multistatic ISAC system based on the mean position method (referred to as Multistatic MPM). We can make following observations about Figure 5: First, it can be straightforwardly noticed that the position estimation error decreases as the number of receiver K increases.

This is because activating more receivers in the proposed sensing cell can estimate sensing objects from various directions and thus improve the position estimation accuracy. Second, it can be observed that when $K = 4$ and 6, the position estimation error in the multistatic ISAC system is smaller than that in the monostatic ISAC system, demonstrating that the multistatic ISAC system with the proposed sensing cell structure outperforms the monostatic ISAC system in position estimation. Third, it can be observed that our proposed estimation method achieves better performance than the mean position method (MPM), showing the effectiveness of the joint data optimization.

We also simulate the CDF and RMSE of position estimation in 26 GHz cellular network as shown in Figure 6. The same conclusions hold again that the multistatic ISAC system with $K = 6$ receivers in the proposed sensing cell structure outperforms monostatic ISAC system. It can also be observed that the position estimation performance in 26 GHz cellular network is better than that in 2.6 GHz cellular network. This is because the sensing area in 26 GHz cellular network is smaller while the system bandwidth is larger compared to that in 2.6 GHz cellular network.

It should be noted that the BSs in both monostatic and multistatic ISAC systems can only estimate a pair of AoA and propagation distance for each object. Therefore, the computational complexity at each receiver in multistatic ISAC system is the same as that in monostatic ISAC system. The only difference is that the computational complexity at the server side of multistatic ISAC system is higher due to the joint data processing using quasi-Newton method. However, the
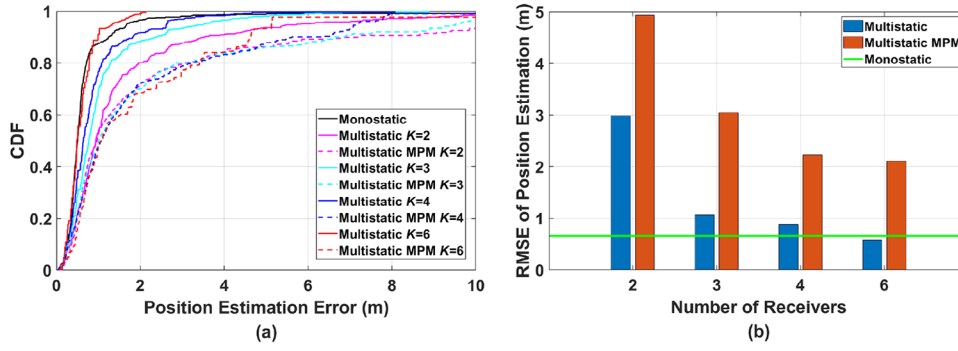
FIGURE 6 Simulated (a) CDF and (b) RMSE of position estimation in the proposed multistatic ISAC system based on 26 GHz cellular network.
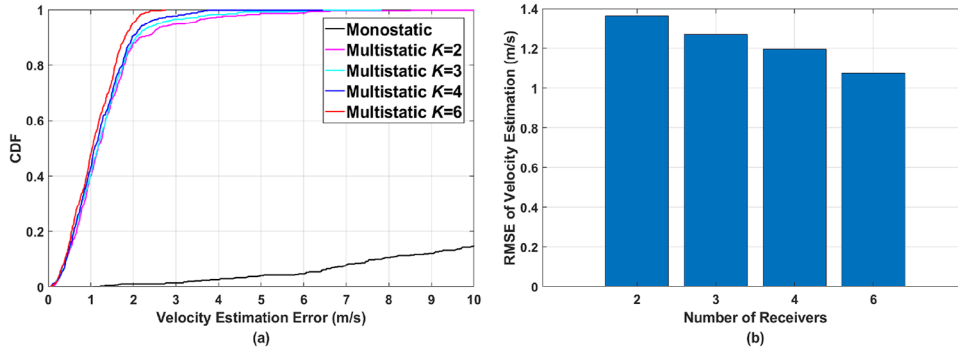
FIGURE 7 Simulated (a) CDF and (b) RMSE of velocity estimation in the proposed multistatic ISAC system based on 26 GHz cellular network.

computing power in the 6G network is envisioned to be greatly enhanced to overcome the issue of increasing computational complexity in our proposed optimization process.

5.2.2 | Velocity estimation performance

We also provide CDF and RMSE results for the velocity estimation in the proposed multistatic ISAC system as shown in Figure 7. It can be observed again from Figures 7a and 7b that the velocity estimation error decreases as the number of receivers K increases. This is not only because more receivers provide much information about the projected velocities, but also related to the reduction of position estimation error. In addition, the velocity estimation error in the multistatic ISAC system is significantly smaller than that in the monostatic ISAC system. The large velocity estimation error in the monostatic ISAC system is caused by the undetectable tangential velocity. These results demonstrate that the proposed multistatic ISAC system can fully recover the velocity of objects by using multiple receivers and overcome the drawbacks of monostatic ISAC system that can only estimate the radial velocity.

To conclude, by implementing multistatic ISAC system in cellular network, the interference power within the network can be greatly reduced. The estimation accuracy of object position and velocity can also be improved when compared with monostatic ISAC system.

6 | CONCLUSIONS

In this paper, we proposed a novel multistatic ISAC system in cellular network. The proposed system well satisfies the ISAC implementation requirement of operators by making use of widely deployed BSs. Specifically in this system, we propose the topology of sensing cell to seamlessly cover cellular network. The sensing results of multiple receive BSs in the sensing cell can be jointly processed with efficient optimization method to estimate position and velocity of sensing objects. In addition, key issues related to this system are also analyzed. It is shown by simulation results that the proposed multistatic ISAC system can efficiently suppress interference power by over 10 dBm for sensing function when compared with the monostatic ISAC system. In addition, the proposed system outperforms the monostatic ISAC system in terms of the estimation error of object position and velocity. These results demonstrated the effectiveness of the proposed multistatic ISAC and the promise of implementing such system in the upcoming 6G mobile network.

This proposed system can serve as an initial guidance in ISAC deployment for operators. For future works, the RCS characteristics of realistic sensing objects can be considered. The reflected signal power to different direction is determined by the RCS distribution over the objects surface. Therefore, further comparisons between multistatic and monostatic ISAC system can be made for typical sensing objects such as unmanned

aerial vehicles. However, multistatic ISAC system can receive reflected signals from various angles, which is beneficial for the estimation of sensing objects.

In addition, the effect of UEs power control on data transmission can also be investigated. The UL power control may be needed for reducing UI and improve sensing performance while this will reduce UL data transmission rate. However, as per Table 2, when there are 500 UEs in each sensing cell of the multistatic ISAC system, UI power is close to MI power so that around 3 dB overall interference power reduction can be achieved by stopping all UL transmissions. Therefore, UL power control with reduced UL data transmission rate has little effect on improving sensing performance. These will be investigated in our future research.

AUTHOR CONTRIBUTIONS

Zixiang Han: Conceptualization; formal analysis; investigation; methodology; software; writing—original draft; writing—review and editing. **Haiyu Ding**: Project administration. **Lincong Han**: Methodology; writing—review and editing. **Liang Ma**: Writing—review and editing. **Xiaozhou Zhang**: Methodology; resources. **Mengting Lou**: Methodology. **Yajuan Wang**: Writing—review and editing. **Jing Jin**: Writing—review and editing. **Qixing Wang**: Funding acquisition. **Guangyi Liu**: Writing—review and editing. **Jiangzhou Wang**: Supervision; writing—review and editing.

CONFLICT OF INTEREST STATEMENT

The authors have declared no conflict of interest.

DATA AVAILABILITY STATEMENT

Data subject to third party restrictions. The data that support the findings of this study are available from China Mobile Research Institute, Beijing 100053, China. Restrictions apply to the availability of these data, which were used under license for this study. Data are available from the authors with the permission of China Mobile Research Institute.

ORCID

Zixiang Han https://orcid.org/0000-0001-7895-0418

REFERENCES

1. Zhang, Z., Xiao, Y., Ma, Z., Xiao, M., Ding, Z., Lei, X., Karagiannidis, G.K., Fan, P.: 6G wireless networks: Vision, requirements, architecture, and key technologies. IEEE Veh. Technol. Mag. 14(3), 28–41 (2019)
2. Saad, W., Bennis, M., Chen, M.: A vision of 6G wireless systems: Applications, trends, technologies, and open research problems. IEEE Network 34(3), 134–142 (2020)
3. Dong, F., Liu, F., Cui, Y., Wang, W., Han, K., Wang, Z.: Sensing as a service in 6G perceptive networks: A unified framework for ISAC resource allocation. IEEE Trans. Wirel. Commun. 22(5), 3522–3536 (2022)
4. Lin, X.: An overview of 5G advanced evolution in 3GPP release 18. IEEE Commun. Stand. Mag. 6(3), 77–83 (2022)
5. Zhang, A., Rahman, M.L., Huang, X., Guo, Y.J., Chen, S., Heath, R.W.: Perceptive mobile networks: Cellular networks with radio vision via joint communication and radar sensing. IEEE Veh. Technol. Mag. 16(2), 20–30 (2020)
6. Cui, Y., Liu, F., Jing, X., Mu, J.: Integrating sensing and communications for ubiquitous IoT: Applications, trends, and challenges. IEEE Network 35(5), 158–167 (2021)
7. Liu, F., Cui, Y., Masouros, C., Xu, J., Han, T.X., Eldar, Y.C., Buzzi, S.: Integrated sensing and communications: Towards dual-functional wireless networks for 6G and beyond. IEEE J. Sel. Areas Commun. 40(6), 1728–1767 (2022)
8. Jiang, H., Mukherjee, M., Zhou, J., Lloret, J.: Channel modeling and characteristics for 6G wireless communications. IEEE Netw. 35(1), 296–303 (2021)
9. Xiong, B., Zhang, Z., Ge, Y., Wang, H., Jiang, H., Wu, L., Zhang, Z.: Channel modeling for heterogeneous vehicular isac system with shared clusters. arXiv preprint, arXiv:2307.07995 (2023)
10. Zhang, J.A., Liu, F., Masouros, C., Heath, R.W., Feng, Z., Zheng, L., Petropulu, A.: An overview of signal processing techniques for joint communication and radar sensing. IEEE J. Sel. Top. Signal Process. 15(6), 1295–1315 (2021)
11. Hua, H., Xu, J., Han, T.X.: Optimal transmit beamforming for integrated sensing and communication. IEEE Trans. Veh. Technol. 72(8), 10 588–10 603 (2023)
12. Temiz, M., Horne, C., Peters, N.J., Ritchie, M.A., Masouros, C.: An experimental study of radar-centric transmission for integrated sensing and communications. IEEE Trans. Microwave Theory Tech. 71(7), 3203–3216 (2023)
13. Lu, S., Liu, F., Hanzo, L.: The degrees-of-freedom in monostatic ISAC channels: NLoS exploitation vs. reduction. IEEE Trans. Veh. Technol. 72(2), 2643–2648 (2022)
14. Pucci, L., Paolini, E., Giorgetti, A.: System-level analysis of joint sensing and communication based on 5G new radio. IEEE J. Sel. Areas Commun. 40(7), 2043–2055 (2022)
15. Barneto, C.B., Riihonen, T., Turunen, M., Anttila, L., Fleischer, M., Stadius, K., Ryynänen, J., Valkama, M.: Full-duplex OFDM radar with LTE and 5G NR waveforms: Challenges, solutions, and measurements. IEEE Trans. Microwave Theory Tech. 67(10), 4042–4054 (2019)
16. Gu, J.-F., Moghaddasi, J., Wu, K.: Delay and Doppler shift estimation for OFDM-based radar-radio (RadCom) system. In: 2015 IEEE International Wireless Symposium (IWS 2015), pp. 1–4. IEEE, Piscataway (2015)
17. Wang, X., Fei, Z., Zhang, J.A., Huang, J.: Sensing-assisted secure uplink communications with full-duplex base station. IEEE Commun. Lett. 26(2), 249–253 (2021)
18. Cui, C., Xu, J., Gui, R., Wang, W.-Q., Wu, W.: Search-free DOD, DOA and range estimation for bistatic FDA-MIMO radar. IEEE Access 6, 15 431–15 445 (2018)
19. Leyva, L., Castanheira, D., Silva, A., Gameiro, A., Hanzo, L.: Cooperative multiterminal radar and communication: A new paradigm for 6G mobile networks. IEEE Veh. Technol. Mag. 16(4), 38–47 (2021)
20. Leyva, L., Castanheira, D., Silva, A., Gameiro, A.: Two-stage estimation algorithm based on interleaved OFDM for a cooperative bistatic ISAC scenario. In: 2022 IEEE 95th Veh. Technol. Conf.:(VTC2022-Spring), pp. 1–6. Helsinki, Finland (2022)
21. Pucci, L., Matricardi, E., Paolini, E., Xu, W., Giorgetti, A.: Performance analysis of a bistatic joint sensing and communication system. In: 2022 IEEE International Conference on Communication Workshops (ICC Workshops), pp. 73–78. IEEE, Piscataway (2022)
22. Kanhere, O., Goyal, S., Beluri, M., Rappaport, T.S.: Target localization using bistatic and multistatic radar with 5g nr waveform. In: 2021 IEEE 93rd Vehicular Technology Conference (VTC2021-Spring), pp. 1–7. IEEE, Piscataway (2021)
23. Zhu, H., Wang, J.: Chunk-based resource allocation in OFDMA systems Part I: chunk allocation. IEEE Trans. Commun. 57(9), 2734–2744 (2009)
24. Zhu, H., Wang, J.: Chunk-based resource allocation in OFDMA systems Part II: Joint chunk, power and bit allocation. IEEE Trans. Commun. 60(2), 499–509 (2012)
25. Willis, N.J.: Bistatic Radar, vol. 2. SciTech Publishing, Chennai (2005)

26. Sturm, C., Wiesbeck, W.: Waveform design and signal processing aspects for fusion of wireless communications and radar sensing. Proc. IEEE 99(7), 1236–1259 (2011)

27. Gill, P.E., Murray, W.: Quasi-Newton methods for unconstrained optimization. IMA J. Appl. Math. 9(1), 91–108 (1972)

28. 3GPP: Requirements for support of radio resource management. 3GPP technical specification TS 38.133 (2021)

29. Li, H., Han, L., Duan, R., Garner, G.M.: Analysis of the synchronization requirements of 5G and corresponding solutions. IEEE Commun. Stand. Mag. 1(1), 52–58 (2017)

30. Li, S., Murch, R.D.: An investigation into baseband techniques for single-channel full-duplex wireless communication systems. IEEE Trans. Wirel. Commun. 13(9), 4794–4806 (2014)

31. Roberts, I.P., Chopra, A., Novlan, T., Vishwanath, S., Andrews, J.G.: Beam-formed self-interference measurements at 28 GHz: Spatial insights and angular spread. IEEE Trans. Wirel. Commun. 21(11), 9744–9760 (2022)